ABSTRACT.
The present paper reviews the recent results achieved in the ICRF-DC experiments performed in helium/hydrogen mixtures in the non-circular tokamaks ASDEX Upgrade and JET and first tests of the ICRF discharges in helium/oxygen mixtures in the circular tokamak TEXTOR. Special emphasis was given to study the physics of ICRF discharges. A new recipe for safe and reliable RF plasma production [$<n_e>$~(3-5)×10^{17} m^{-3}, T_e~(3-5) eV] with improved antenna coupling efficiency (by 1.5-3 times) and improved radial/poloidal homogeneity was proposed and successfully tested: coupling the RF power in the FW-IBW mode conversion scenario in plasmas with two ion species. The first results on ICRF wall conditioning in helium/hydrogen and in helium/oxygen mixtures are analyzed.

1. INTRODUCTION

To apply the wall conditioning procedure in the future superconducting fusion reactors like ITER in between shots, only discharges fully compatible with the presence of a permanent high magnetic field can be used. The alternative ICRF Discharge Conditioning (ICRF-DC) technique was proposed and developed on the circular tokamaks TEXTOR, TORE SUPRA and HT-7. The technique demonstrated complete compatibility with the toroidal magnetic field, high wall conditioning efficiency [1-4] and was proposed for between-pulse conditioning in ITER [5]. The encouraging efficiency of the wall conditioning achieved on limiter tokamaks stimulated next steps in the development of the ICRF-DC on divertor tokamaks [6]. In this paper, the physics of ICRF discharge and the recent results achieved on ASDEX Upgrade, JET and TEXTOR are discussed.

2. ICRF-DC CHARACTERIZATION

The ICRF-DC experiments on reviewed tokamaks have been performed using the standard ICRF systems without any modifications in hardware and under the conditions mentioned elsewhere [1-6].

3. NEUTRAL GAS RF BREAKDOWN

The initiation of ICRF discharge in a toroidal magnetic field B_T results from the absorption of RF energy mainly by electrons [7,8]. The RF $\tilde{E}_z$-field (parallel to the B_T-field) is thought to be responsible for this process. In the general case of a poloidal loop-type ICRF antenna with a tilted Faraday shield (FS), the RF $\tilde{E}_z$-field in vacuum can be induced *electrostatically* and *inductively* [8]. However, in the ICRF band for the present-day fusion devices (~10-100 MHz), for most of the antenna κ_z-spectrum, the RF waves cannot propagate in the vacuum vessel: $\kappa_\perp^2 = \omega^2/c^2 - \kappa_z^2 < 0$, where $\kappa_\perp$ is the perpendicular wave-vector. Hence, the neutral gas breakdown and initial ionization may only occur locally at the antenna-near $\tilde{E}_z$-field (evanescent in vacuum). To avoid deleterious effects of the neutral gas breakdown and arcing inside the antenna box, the frequency of RF generators and the RF voltage/power at antenna straps were reduced to minimal values, while still meeting the requirements for ICRF breakdown outside of the antenna box [8]. Figure 1 shows the transition from the RF breakdown phase to the ICRF discharge phase in JET. It is clearly seen that the gas

breakdown occurs after some delay and shows up in a drop in the antenna RF voltage (averaged over four radiating straps) and in a burst in the H_α emission (measured toroidally at ~130° away from the antenna port).

From the point of view of ICRF system operation, such a correlation is the sign of RF discharge initiation outside of the antenna box and subsequent propagation of the initial low-density plasma ($w \geq w_{pe}$, $n_e(r) \leq 1.4 \times 10^{13}$ m^{-3} for $f = 33.9$MHz) along the magnetic field lines. The pressure dependence of the neutral gas breakdown time (associated with the RF voltage drop and the occurrence of the initial peak in the H_α emission) is plotted in Fig.2. Data from three tokamaks (TEXTOR, AUG and JET) were found to be in good agreement for the similar RF voltages (~8-13kV), frequencies (~30-34MHz) and the same pressures. It may be an indication that the antenna RF voltage (the antenna-near $\tilde{E}_z$ electric field) plays a fundamental role in the neutral gas breakdown and that the breakdown time is independent of the machines size.

4. ICRF PLASMA BUILD-UP

After the first (gas local breakdown) phase of the RF discharge, as ω_{pe} becomes of the order of ω, plasma waves can start propagating in a relay-race regime governed by the antenna κ_z-spectrum. The collisional absorption of the waves (T_e~3-5 eV during the ionization phase [3,8]) stimulates further space ionization of the neutral gas and plasma build-up in the torus (plasma phase). Such a non-resonant coupling allows RF plasma production at any B_T [8]. However, at plasma densities below a threshold for the FW propagation, coupling efficiency of the poloidal antennas is rather low in plasmas with a single ion species, $\eta = (R_{ant} - R_{loss}) / R_{ant}$ ~ 20-30%. It results in the RF plasma build-up mainly at the machine low field side, LFS (antennas side) [6]. Both, antenna coupling and plasma homogeneity could be dramatically improved when a gas mixture of $H_2/(He+H_2)$ ~ 0.1-0.3 was used (Figs.3,4).

In the AUG case, the improved performance was achieved when the ICR layer $\omega=\omega_{cH}$ and the nearby FW-IBW mode conversion layer were shifted to the LFS. As a result, the antenna coupling efficiency increased up to 3 times at $f = 30.0$ MHz (Fig.3). In the JET case, the radial extension of RF plasmas towards the HFS was clearly seen from the multi-channel FIR interferometer data (Fig.4). This effect has been predicted from the electron energy deposition profiles calculated with the 1D RF code [9] for helium RF plasmas with different H concentrations.

Analysis of the core atomic spectroscopy and the VUV spectroscopy data showed appearance of the H_α, D_α and *HeI* (neutral) lines during the JET ICRF discharges. Assuming an equilibrium (coronal) ionization balance, T_e~2-5 eV was derived from the ionization stages observed for shots at the gas pressure $p_{tot} \approx (2\text{-}6)\times10^{-3}$ Pa.

All ICRF-DC experiments performed until now reported on the generation of high-energy fluxes of H (with energies up to 60keV) and of D atoms (up to 25keV), which were detected by a neutral particle analyzer (NPA) [3,6,8]. Clear evidence of tail formation in the distribution functions of H and D atoms was observed at higher ion cyclotron harmonics ($\omega = 2\omega_{cH} = 4\omega_{cD}$). This fact may be

understood in terms of RF quasilinear diffusion: ion cyclotron harmonic heating tends to accelerate the faster particles more, with tail formation at higher energy than for fundamental heating [10].

5. ICRF WALL CONDITIONING TESTS

One of the major issues in ITER is the retention of tritium in re-deposited carbon layers. The removal of hydrocarbon layers by oxygen is considered as the most promising method. Directly related pilot experiments have successfully been performed on TEXTOR, addressing ICRF discharge initiation and *a-C:H*-film removal in the O_2/He mixtures. The mass-spectrum analysis of the residual gas revealed that injected oxygen was converted into *CO* and CO_2 (Fig.5). The estimated *C*-erosion rate was ~0.13 nm/s assuming to be homogeneous over whole vessel area. In the AUG case, the conditioning efficiency was found higher in the H_2/He mixtures compared with the pure helium gas (Fig.6) due to better both antenna coupling and plasma homogeneity.

ACKNOWLEDGEMENTS

This work has been performed under the European Fusion Development Agreement.

REFERENCES

[1]. H.G. Esser, et al., *Journal of Nuclear Materials* 241-243 (1997) 861-866.

[2]. A. Lyssoivan, et al., in *14th Topical Conf. on Radio Frequency Power in Plasmas, Oxnard 2001,* AIP Conf. Proceedings 595, New York 2001, p.146-149.

[3]. E. de la Cal and E. Gauthier, *Plasma Phys. Control. Fusion* **39** (1997) 1083-1099.

[4]. J.K. Xie, et al., *Journal of Nuclear Materials* 290-293 (2001) 1155-1159.

[5]. ITER Physics Guidelines, N19 FDR 1 01-07 13R0.1, (2001), pp.109-110.

[6]. A. Lyssoivan, et al., *Journal of Nuclear Materials* 337-339 (2005) 456-460.

[7]. M.D. Carter, et al., *Nuclear Fusion* **30** (1990), pp.723-730.

[8]. A. Lyssoivan, et al., *Final Report on ITER Design Task D350.2, LPP-ERM/KMS* 114 (1998).

[9]. D.Van Eester and R.Koch, *Plasma Phys. Control. Fusion* **40**, 1949-1975 (1998).

[10]. R. Koch, Transactions of Fusion Sciens and Technology **45** (2004) 203-210.

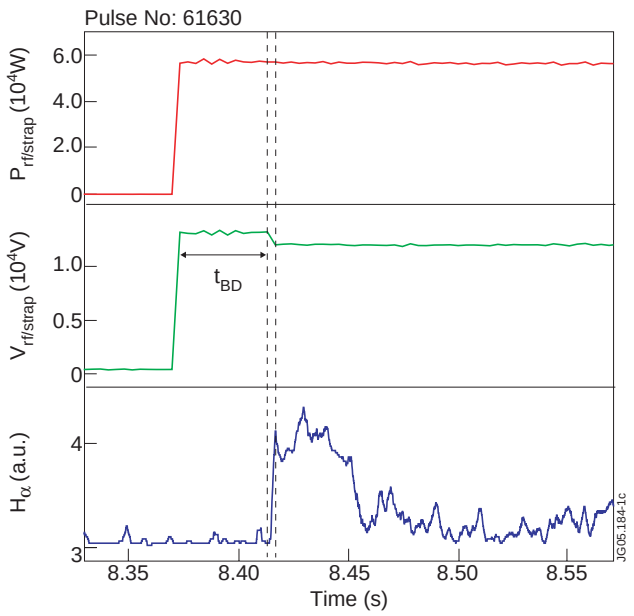

Figure 1: The transition from the neutral gas breakdown phase ($\omega \geq \omega_{pe}$) to the ICRF discharge phase ($\omega \geq \omega_{pe}$) in JET.

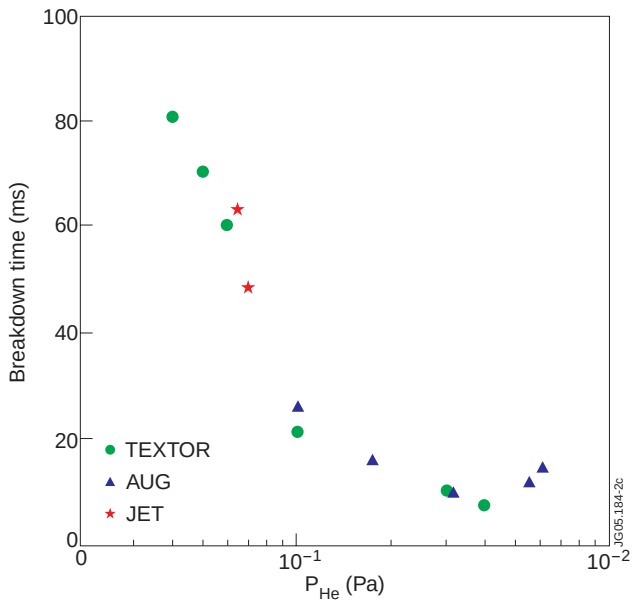

Figure 2: Pressure dependence of the RF breakdown time derived from the V_{RF} and H_α emission signals ($P_{RF/ant.strap} \approx$ 30-50 kW, $f \approx 30$ MHz, $\omega = 4\omega_{cHe+} = 2\omega_{cD} = \omega_{cH}$), after [6].

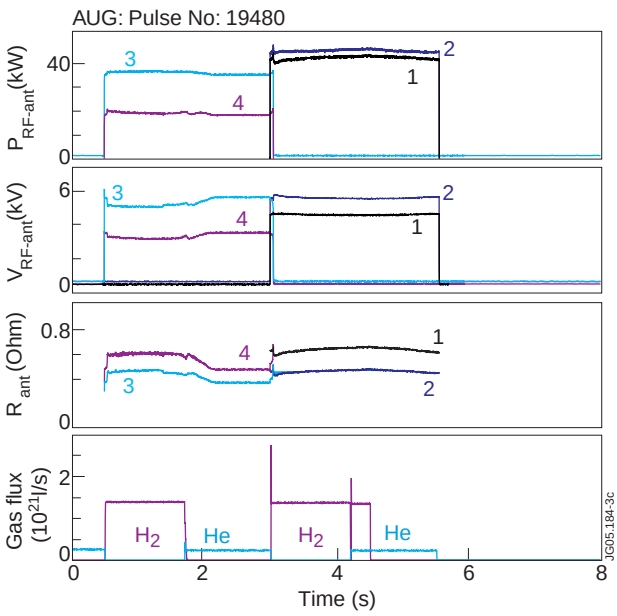

Figure 3: Effect of hydrogen/helium mixture on antenna coupling in AUG: $f_{ant3} = f_{ant4} = 30.0$MHz, $f_{ant1} = f_{ant2} = 36.5$MHz, $B_T = 2.35$T

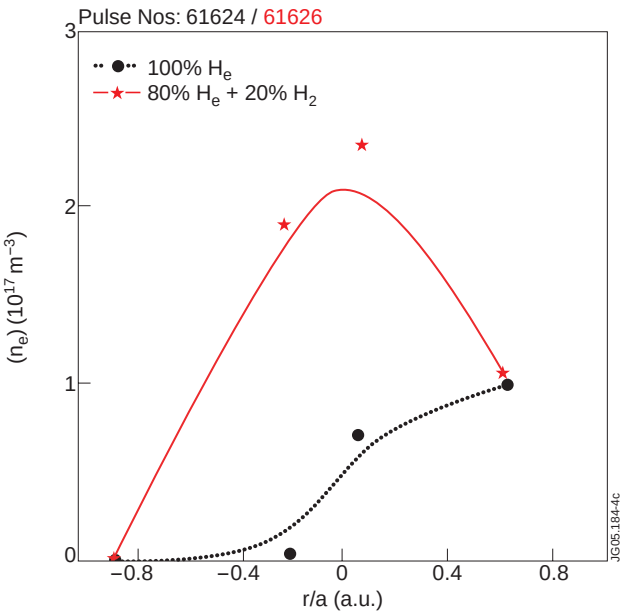

Figure 4: The line-averaged plasma density profiles for two ICRF discharges in JET: in pure helium (dashed) and in a gas mixture of $H_2/(He + H_2)$~0.2 (solid), $P_{RF-pl} \approx$ 70kW, $f = 33.9$MHz, $B_T = 2.45$T.

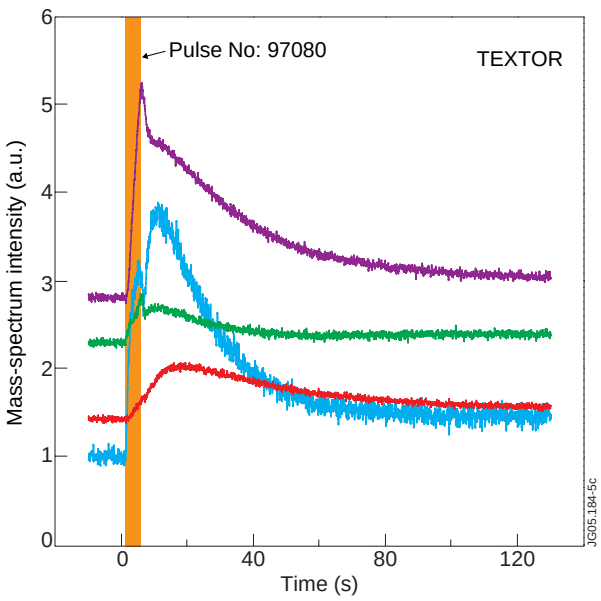

Figure 5: ICRF-DC in the O_2/He mixture in TEXTOR: $P_{RF\text{-}pl} \approx 50$ kW, f=29.0 MHz, B_T=2.3 T, He-flow, O_2-puff (15.8 mbar l during RF pulse).

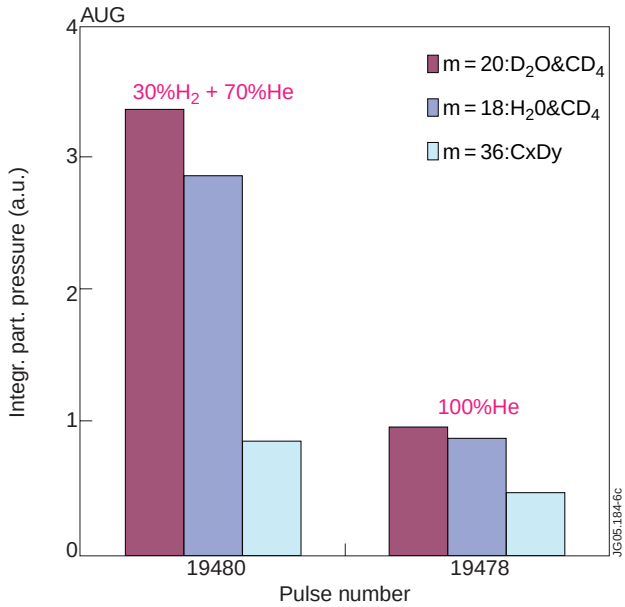

Figure 6: Effect of ICRF-DC in AUG in helium/hydrogen mixture (Pulse No: 19480, $P_{RF\text{-}pl} \approx 50$kW) and in pure helium (Pulse No: 19478, $P_{RF\text{-}pl} \approx 30$kW).